Available online at www.sciencedirect.com

SCIENCE DIRECT®

ELSEVIER

Dyes and Pigments 63 (2004) 191–202

DYES and PIGMENTS

www.elsevier.com/locate/dyepig

New push–pull type dendritic stilbazolium dyes: synthesis, photophysical and electrochemical investigation

Amaresh Mishra*, Nanda S. Haram

Department of Chemical Sciences, Tata Institute of Fundamental Research,
Homi Bhabha Road, Colaba, Mumbai 400 005, India

Received 21 October 2003; received in revised form 12 December 2003; accepted 20 February 2004

Abstract

The synthesis of some dendritic tri- and tetra-chromophoric solvatochromic stilbazolium dyes is presented. The dyes were characterized by ^{1}H, ^{13}C NMR and mass spectroscopy. The UV–Vis and steady-state fluorescence spectroscopic investigation shows a solvatochromic absorption and emission, which result from the intramolecular charge transfer (ICT) nature of the chromophores present in the dendritic structure (**1**–**4**). The fluorescence decay was fitted to bi-exponential in all the solvents. Systematic variation of fluorescence quantum yield and lifetime in organic solvents were observed. In chloroform and dichloromethane, these dyes show intense fluorescence and the fluorescence lifetime is also high, which is due to specific interaction of the dye with solvent. Using cyclic voltammetry (CV) experiments, the electrochemical response of the dyes and electronic interactions between the electroactive sites of these dendritic constructs were explored. CV responses of these dyes (**3**, **4a** and **4b**) show three successive, well-separated reduction peaks, which indicate strong electronic coupling between the chromophoric units.

Keywords: Stilbazolium (hemicyanine) dyes; Dendritic; Absorption and emission spectra; Fluorescence lifetime; Cyclic voltammetry; Electronic coupling

1. Introduction

Stilbazolium dyes (family of cyanine dyes) are an important class of materials that can be synthetically tailored to address specific chemico-physical needs. Thus, a large number of conjugated organic chromophores of donor–acceptor type have been synthesised and studied by various techniques [1]. The design and construction of these molecular and supramolecular photoactive materials have been actively pursued in recent years, due to their potential applications in opto-electronic and photoswitchable molecular devices [2], information processing and storage devices [3] and in non-linear optics [4]. Such dyes are very sensitive to medium polarity and rigidity (viscosity) and thus can be used as luminescent probes in micelles [5], membranes and biological systems [6].

Monochromophoric dimethylaminostyryl pyridinium (DASP) dye in various solvents revealed

---

* Corresponding author. Tel.: +91-22-2280-4545; fax: +91-22-2280-4610.

E-mail address: amishra@tifr.res.in (A. Mishra).

0143-7208/$ - see front matter © 2004 Elsevier Ltd. All rights reserved.
doi:10.1016/j.dyepig.2004.02.011

that there exist two resonance structures. The structure of the dye can be pictured as a compromise between two resonance forms: the benzenoid form and quinoid form [7,8]. In the ground state, the benzenoid form dominates while the quinoid form dominates in the first excited state. Even though the benzenoid and quinoid forms are mesomeric resonance structures, it can be seen that the positive charge resides on different nitrogen atoms in the two structures, i.e. on pyridinium nitrogen in benzenoid form and on amino nitrogen in quinoid form. As a result, depending on the solvent polarity, the solvents may interact differently with the two forms. So in nonpolar solvent, the quinoid form dominates whereas the benzenoid form is stable in polar solvent [9]. As seen in the literature, the quinoid form was proposed to be quasi-stable in the ground state [10] and stable in the excited state [11]. The electronic transition is thus accompanied by significant changes in the length of the central double bond (–C=C–) and the single bonds (–C–ϕ) connecting the ethylene group to the aniline and pyridyl ring for these two forms [12].

These dyes having flexible donor–acceptor type moieties, upon photoexcitation undergo internal rotation about the single bond, leading to the formation of twisted intramolecular charge transfer (TICT) state [13,14]. Ephardt and Fromherz [15] proposed the TICT state formation to explain the fluorescence of stilbazolium dye in different solvents. From the recent quantum chemical calculations, solvation and other experimental studies of DASP dye, it has been shown that rotation of aniline moiety is responsible for the ultrafast nonradiative decay (TICT state) process [13,16]. With increase in solvent polarity of the medium the activation barrier of the twisted ICT state decreases which decreases the fluorescence quantum yield. Thus, the fluorescence originates generally from a non-TICT (locally excited, LE) state. Due to their strong intramolecular charge transfer character, these dyes show characteristically broad and structureless absorption and emission spectra with large Stokes shift, especially in polar solvents. A consequence of the above photophysical properties of the stilbazolium dye is the likely utility in nonlinear optical and sensor applications. Synthesis of dendritic structures containing these dyes has not been reported.

Herein, we present the synthesis of some new and novel multichromophoric dendritic stilbazolium dyes (Fig. 1) along with their spectroscopic and electrochemical properties. To our knowledge, dendritic stilbazolium dyes that display strong electronic communication between them have not been reported before.

2. Results and discussion

2.1. Synthesis

Dyes **1** and **2** were synthesised by the reaction of tetrakis(5-bromo-2-oxabutyl)methane with four equivalents of γ-picoline followed by Knoevenagel condensation with appropriate aldehydes [17]. Reduction of 1,3,5-tricarboxybenzene ($BH_3{\cdot}THF$) (Scheme 1) was confirmed (^{13}C NMR) by the disappearance of peak at 178.4 ppm assigned to the COOH moiety and the appearance of a new peak at 63.47 ppm attributed to the formation of the CH_2OH group. Conversion (CH_3SO_2Cl, Et_3N) to the corresponding trimesylate **7** was similarly characterized (^{13}C NMR) by the disappearance of the peak at 63.47 ppm (CH_2OH) and the appearance of new peak at 36.7 (CH_3) and 69.35 (OCH_2), as well as the expected methyl absorption (^1H NMR) at 2.87 ppm. Conversion of **7** to the tribromide **8** (NaBr, DMF) was subsequently monitored (^{13}C NMR) by the observation of the disappearance of the peaks at 36.7 and 63.47 ppm (CH_3 and OCH_2, respectively) and the peak (^1H NMR) at 2.87 ppm (CH_3) and the appearance of new signal (^{13}C NMR) at 32.41 ppm (CH_2Br). A peak at m/z 355 ($M^+ + H$, calcd. 353.82) in ESI-MS provides further proof of tribromide structure. The core tribromide **8** then treated with γ-picoline, and subsequently, condensed with *N*,*N*-dimethyl aminobenzaldehyde and *N*,*N*-dihexadecyl aminobenzaldehyde [17] by Knoevenagel reaction to afford, respectively, the corresponding dyes **3** and **4a** as red solid (Scheme 2). Dye **4b** was synthesised by the reaction of **4a** with excess of sodium tetraphenylborate in methanol. The melting points

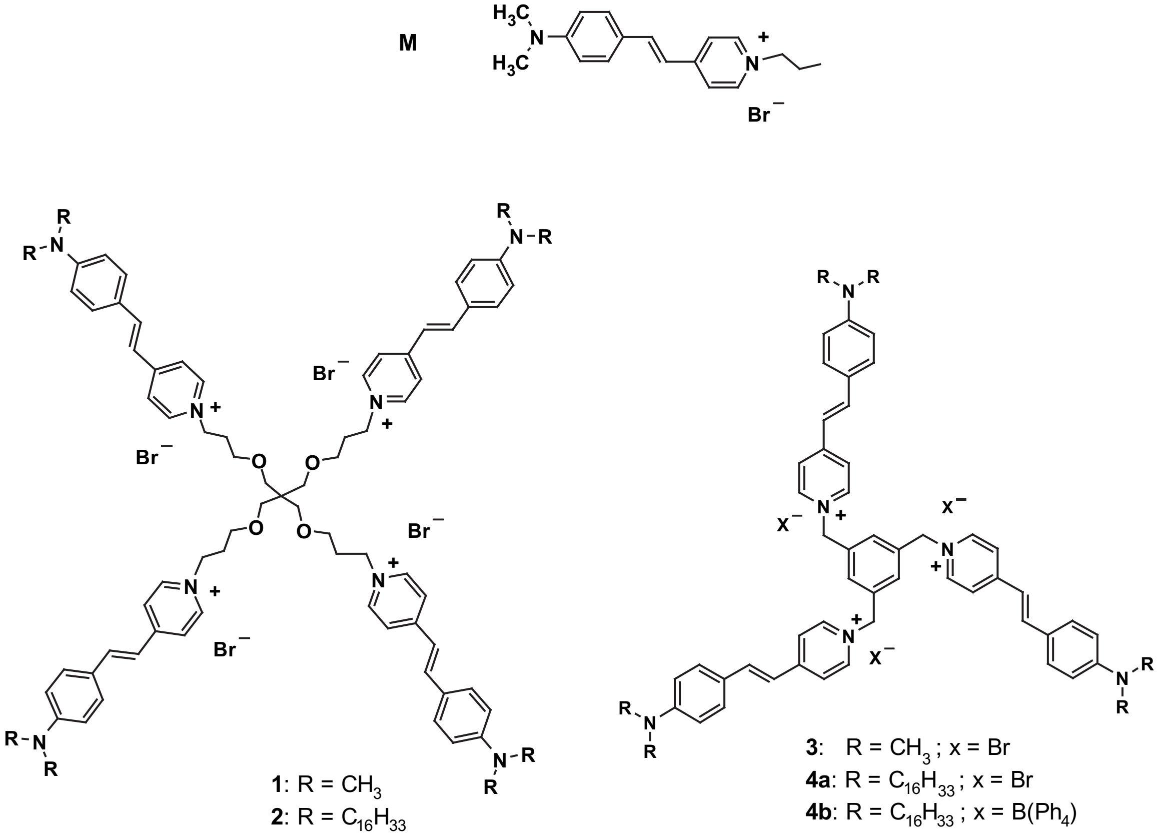

Fig. 1. Schematic representation of the dyes.

for compounds **4a** and **4b** are not sharp, these could be attributed to the liquid crystal properties of the hemicyanine dyes. The dyes were purified by crystallization from appropriate solvent mixtures (see Section 3). Generally, 2–3 crystallizations were required for obtaining a constant value of molecular extinction coefficient. The structure and purity of the prepared compounds were confirmed by NMR, mass spectroscopy and thin layer chromatography. Based on the large coupling constant for the olefinic protons ($J_{trans} = 15$–16 Hz) it is concluded that these dyes adopt an all-*trans* conformation in the ground state, which minimizes the steric interactions in the chromophores. The ESI mass spectra of the dyes show most stable base peak at *m*/*z* 225, 725.9 and 726 for **3**, **4a** and **4b**, respectively, and other charged fragments, which are given in detail in Section 3.

2.2. Spectroscopic studies of dyes 1–4

2.2.1. Absorption spectra

The spectra of dendritic dyes **1**–**4** were measured in several organic solvents (Table 1). The results show high solvatochromic shift. Among the alcoholic solvents these dendritic dyes show red shift in absorption spectra as compared to blue shift in monochromophoric dye (**M**) [7]. The high intensity broad absorption band corresponds to the $S_1 \leftarrow S_0$ state due to intramolecular charge transfer (ICT) from electron-donating dialkylamino group to electron accepting pyridinium moiety. Fig. 2 shows the absorption spectra of dyes **1**–**4** in ethanol. **M** with *N*,*N*-dimethylamino group shows absorption maximum at 479 nm in methanol [7]. Relative to the monomer **M**, a red shift in the absorption maxima (7–33 nm) was observed for dyes **1**–**4** in methanol. Depending on the solvents,

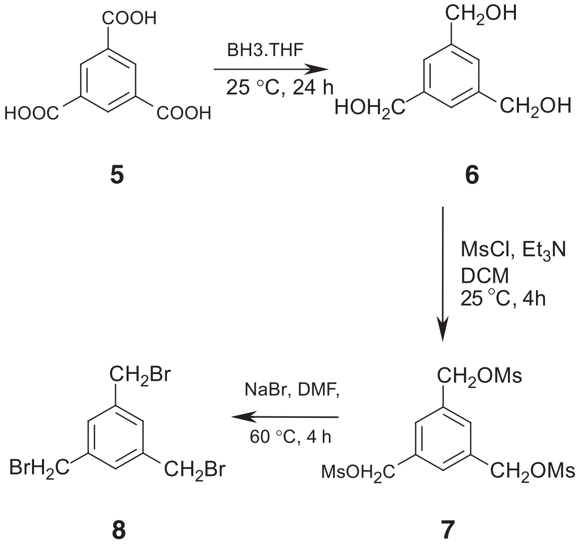

Scheme 1.

the extinction coefficient (ε) value of this transition ranges between 110,000 and 199,000 $\mathrm{M}^{-1}\,\mathrm{cm}^{-1}$ for **1** and **2**, which is 3–3.5 times higher than **M**; whereas, **3**, **4a** and **4b** have almost similar or smaller ε values than **M** (Table 1).

The change in alkyl chain lengths of *N*-alkyl group in aniline moiety of the dye (**1** vs. **2** and also **3** vs. **4**) shows a progressive effect on the absorption spectral peak. The absorption maxima show bathochromic (red) shift with change in alkyl group from C1 to C16. This phenomenon might be attributed to the electron-donating ability of the nitrogen, which increases as the length of the alkyl chain increases due to inductive effect of alkyl group. It has been suggested that, the bathochromic shift with increase in alkyl chain length at the amino nitrogen is due to the increase in delocalisation of the lone-pair electron at the nitrogen to the π-orbital of the dye chromophore cation [18].

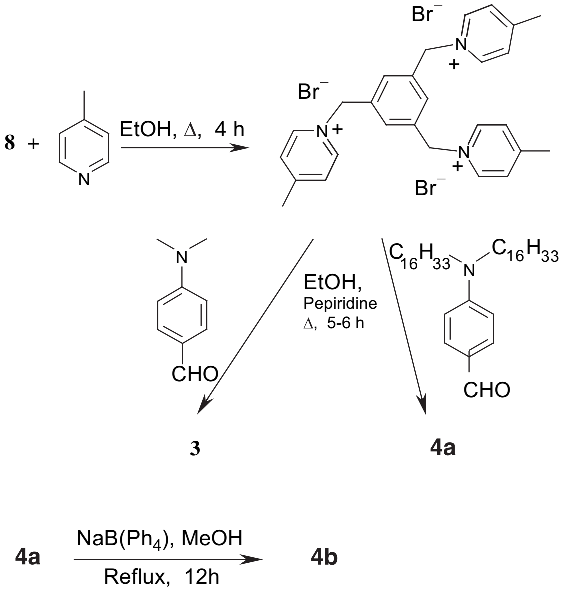

Scheme 2.

In the organic solvents, dendritic tetra-chromophoric dye **1** shows small variation in the absorption maximum, which ranges from 460 nm (1,4-dioxane) to 489 nm (dichloromethane) as compared to monochromophoric dye **M**, where the shift ranges from 463 nm (1,4-dioxane) to 513 nm (dichloromethane) (see Table 1). Dye **2** shows a range from 471 nm (1,4-dioxane) to 511 (dichloromethane) with an increase of 11–22 nm as compared to **1**. In nonpolar solvents **2** shows absorption at 482 nm (aromatic solvents) and 475 nm (hexane). Dye **1** was not measured in nonpolar solvents due to poor solubility.

Interestingly, dye **3** shows bathochromic shift of 10–15 nm compared to **1** in all the solvents. The red shift for dye **3** may be accounted for the presence of benzene ring at the core, which promotes strong electronic coupling between the chromophoric units. The electronic coupling is absent in dye **1** in which, the chromophores are separated by long alkyl (ether) spacer group. Dyes **4a** and **4b** also show bathochromic shift as compared to **2** (having similar alkyl group) in all solvents, which is ascribed to the above mentioned electronic coupling. This strong electronic coupling between the chromophores for dyes **3**, **4a** and **4b** was also seen in electrochemical study of these dyes, which is discussed later.

The plot of absorption wavelength vs. Reichardt's $E_T(30)$ solvent polarity parameter [19] (Fig. 3) shows that there is a correlation among all the solvents except $CHCl_3$ [$E_T(30) = 39.1$] and CH_2Cl_2 [$E_T(30) = 40.7$]. This correlation can be assigned to nonspecific interaction of solvent and the dipole moment of the dye molecule. The significant deviation in chloroform and dichloromethane

Table 1
Absorption and emission spectral data of the dyes (**1**–**4**) under study (polar and nonpolar solvents are separated by a solid line)

Solvents	$E_T(30)$	**M**			**1**			**2**			**3**			**4a**			**4b**		
		λ_{max}/nm ($\varepsilon\times10^{-5}$) M^{-1} cm^{-1}	λ_{em} (nm)	Stokes shift (cm^{-1})	λ_{max}/nm ($\varepsilon\times10^{-5}$) M^{-1} cm^{-1}	λ_{em} (nm)	Stokes shift (cm^{-1})	λ_{max}/nm ($\varepsilon\times10^{-5}$) M^{-1} cm^{-1}	λ_{em} (nm)	Stokes shift (cm^{-1})	λ_{max}/nm ($\varepsilon\times10^{-5}$) M^{-1} cm^{-1}	λ_{em} (nm)	Stokes shift (cm^{-1})	λ_{max}/nm ($\varepsilon\times10^{-5}$) M^{-1} cm^{-1}	λ_{em} (nm)	Stokes shift (cm^{-1})	λ_{max}/nm ($\varepsilon\times10^{-5}$) M^{-1} cm^{-1}	λ_{em} (nm)	Stokes shift (cm^{-1})
MeOH	55.4	479(0.55)	579	3605	486(1.41)	608	4128	499(1.82)	615	3780	498(0.25)	618	3899	509(0.30)	624	3621	513(0.36)	629	3595
EtOH	51.9	484(0.55)	576	3300	484(1.64)	604	4104	499(1.7)	613	3727	498(0.28)	613	3767	508(0.60)	621	3582	517(0.49)	625	3342
1-Propanol	50.7	487(0.57)	576	3172	482(1.60)	602	4136	497(1.72)	608	3674	495(0.27)	611	3836	508(0.65)	617	3478	516(0.49)	622	3303
1-Butanol	49.7	490(0.63)	576	3047	480(1.58)	600	4167	494(1.74)	607	3769	491(0.27)	608	3919	507(0.67)	612	3383	513(0.51)	617	3286
2-Propanol	48.4	485(0.54)	571	3105	479(1.58)	600	4210	489(1.85)	604	3893	490(0.25)	607	3933	506(0.70)	613	3476	518(0.54)	618	3086
1-Octanol	48.1	–	–	–	475(1.51)	594	4217	492(1.86)	599	3630	489(0.26)	595	3643	498(0.64)	589	3143	508(0.53)	600	3018
DMSO	45.1	476(0.48)	589	4030	479(1.44)	621	4773	487(1.11)	625	4534	491(0.30)	627	4417	486(0.55)	615	4316	486(0.44)	624	4550
CH_2Cl_2	40.7	513(0.54)	560	1636	489(1.35)	597	3699	511(1.74)	612	3229	500(0.33)	600	3333	516(0.61)	606	2878	545(0.6)	624	2323
$CHCl_3$	39.1	496(0.60)	560	2304	489(1.55)	585	3355	505(1.99)	599	3107	500(0.29)	580	2758	514(0.59)	587	2419	539(0.53)	606	2051
1,4-Dioxane	36.0	463(0.50)	557	3644	460(1.48)	576	4568	471(1.35)	586	4166	480(0.30)	580	3592	482(0.49)	578	3446	518(0.55)	606	2803
Benzene	34.3	477(0.63)	552	2848	–	–	–	482(1.04)	594	3911	–	–	–	484(0.46)	562	2868	529(0.46)	604	2347
Toluene	33.9	–	–	–	–	–	–	482(1.61)	593	3882	–	–	–	483(0.56)	559	2677	529(0.63)	603	2320
p-Xylene	33.1	–	–	–	–	–	–	483(1.49)	593	3840	–	–	–	483(0.57)	556	2718	527(0.60)	602	2364
n-Hexane	31.0	–	–	–	–	–	–	475(1.62)	598	4330	–	–	–	481(0.45)	630	4917	508(0.58)	620	3556

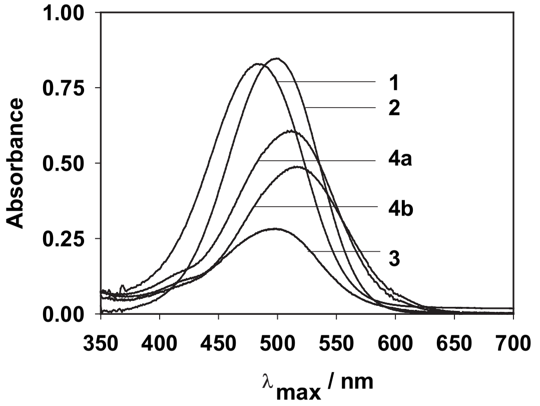

Fig. 2. Absorption spectra of dyes **1**–**4** in ethanol. Dyes **1**, **2**, **3** contain 1% MeOH in solution but dyes **4a** and **4b** contain 2% $CHCl_3$ in all solvents. [Dye] = 10 μM.

indicates a specific interaction between the dye and the solvent.

2.2.2. Emission spectra

Like absorption spectra, these dyes also show broad and structureless emission spectra with large Stokes shifts. The emission data are given in Table 1. The steady-state fluorescence emission spectrum of dye **4a** in chloroform, toluene and ethanol is given in Fig. 4. The Stokes shift ($\Delta\nu$) is an important characteristic of change of dipole moment upon excitation and thus indicates the extent of charge transfer in the excited state [20]. A large Stokes shift in these chromophores generally, is

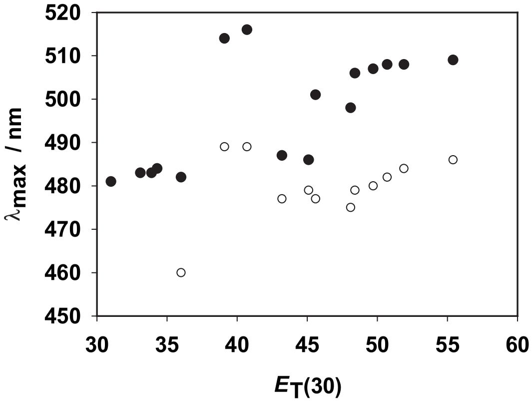

Fig. 3. The representative plot of absorption maxima vs. empirical solvent polarity scale $E_T(30)$ for dyes **1** (○) and **4a** (●).

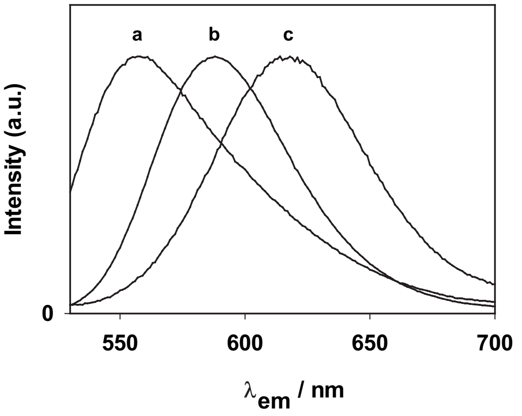

Fig. 4. Representative fluorescence emission spectra of dye **4a** in (a) toluene, (b) chloroform and (c) ethanol excited at their respective absorption maxima. [Dye] = 10 μM.

Table 2
Quantum yield of dyes **1**–**4** measured in various solvents

Solvents	η[a]	$\phi_f(\times 10^{-3})$				
		1	**2**	**3**	**4a**	**4b**
MeOH	1.326	2.43	5.69	7.69	8.26	15.1
EtOH	1.359	3.17	13.6	14.08	17.01	18.6
1-Propanol	1.385	19.7	41.8	42.35	27.6	43.43
1-Octanol	1.427	71.6	215.4	95.02	80.2	82.6
$CHCl_3$	1.443	68.7	148.0	128.8	92.4	135.1
CH_2Cl_2	1.421	41.9	73.01	61.2	54.03	47.7

[a] η = Refractive index of the solvent.

ascribed to a different charge distribution in the excited state and the ground state of the molecule. In these molecules, the positive charge is transferred from pyridinium nitrogen (benzenoid form) to dimethylamino group (quinoid form), thereby increasing the dipole moment. Dipolar aprotic solvent (DMSO) shows large shift in emission band with a large Stokes shift (>4300 cm^{-1}). The general variation of emission spectra with solvents are similar to those observed in absorption spectra for all the dyes.

The dendritic dyes described here are tri and tetra cationic in nature. Solubility of dyes **1** and **3** is very poor in nonpolar solvents. However, dyes **2**, **4a** and **4b** are soluble in nonpolar solvents because of C16 alkyl chain. An interesting emission behavior for dyes **2** and **4a** is observed in the highly nonpolar solvent, *n*-hexane, compared to other nonpolar solvents (benzene and dioxane) of similar dielectric constant (Table 1). The absorption and emission spectral shift is marginal for dye **2** among nonpolar solvents. However, the emission for dye **4a** (and **4b**) in *n*-hexane are red shifted by another 70 nm (and 16 nm) compared to benzene. This is difficult to explain based on the polarity factor alone. We speculate that the strength of electronic coupling between chromophores in dyes **4a** and **4b** may be different in *n*-hexane and aromatic solvents.

These dyes show very low fluorescence quantum yield (Table 2) in organic solvents. This fact may be attributed to the ultrafast internal twisting process in the excited state of the molecule [10,21,22]. It has also been reported that with increase in solvent polarity the quantum yield of monochromophoric hemicyanine dyes decreases [23]. The low yield of the dyes in methanol to propanol in comparison with 1-octanol can be associated not only with the solvent viscosity (which restricts the TICT state formation) but also with the polarity of the solvent. High quantum yield in chlorinated solvents may be due to the restriction in the formation of the TICT state, because of some specific interaction.

To understand more about the excited state dynamics, fluorescence decay lifetimes of the dyes were measured in some representative solvents. The fluorescence decays were fitted to a bi-exponential in all the solvents. The lifetimes of these dyes are very short in alcoholic (ethanol, 1-propanol) solvents (Tables 3 and 4). Fig. 5 shows fluorescence decay of dye **4a** in ethanol and chloroform. The fluorescence decay of these dyes in chloroform is much slower than in ethanol. From a kinetic model, Bohn et al. [24] have proposed that during reversible coupling between an emissive state and another electronic excited state (TICT state), single-exponential decay cannot be observed and the fluorescence decay is expected to follow a double-exponential. As reported earlier [13], a high polarity and low viscosity solvent is more favorable for nonradiative TICT state formation. In our study, it has been found that the variation of quantum yield in the organic solvents is the same as variation of the lifetime. The difference in the quantum yield and lifetime values is

Table 3
Time resolved fluorescence decay of dyes **1** and **2** in organic solvents

Solvents	**1**				**2**			
	η_1 (ns) (α_1)	τ_2 (ns) (α_2)	τ_{avg} (ns)	χ^2	τ_1 (ns) (α_1)	τ_2 (ns) (α_2)	τ_{avg} (ns)	χ^2
MeOH	0.19(0.24)	0.06(0.76)	0.09	1.32	0.1(0.24)	0.01(0.76)	0.03	1.24
EtOH	0.21(0.28)	0.07(0.72)	0.11	1.30	0.1(0.20)	0.03(0.80)	0.05	1.30
1-Propanol	0.24(0.32)	0.15(0.68)	0.18	1.41	0.43(0.26)	0.19(0.74)	0.25	1.88
1-Octanol	0.65(0.45)	0.34(0.55)	0.48	1.06	1.24(0.44)	0.69(0.56)	0.93	1.02
$CHCl_3$	0.69(0.46)	0.26(0.54)	0.46	1.04	1.25(0.54)	0.65(0.46)	0.97	1.06
CH_2Cl_2	0.42(0.54)	0.17(0.46)	0.31	1.12	0.67(0.74)	0.20(0.26)	0.55	0.96

therefore attributed to the change in nonradiative rates. The plot of ϕ_f vs. τ_{avg} (Fig. 6) is compatible with an almost linear relationship irrespective of the solvent.

2.2.3. Aggregation of dyes in organic solvents

The dendritic dyes reported are ionic in nature and hence solubility in polar solvents including water is expected to be good. On the other hand, the dyes **2**, **4a** and **4b** contain hydrophobic hexadecyl alkyl chain, two per chromophore. As a result of this, one would expect surfactant or lipid like aggregation behavior of the dendritic dyes. The spectroscopic data shown in Table 1 are for solvents where the solubility of the dye is high, the dye solution is stable and no aggregation behavior is indicated. The dyes do show aggregation behavior in some solvents. For example, **2**, **4a** and **4b** are almost insoluble in water because of the multiple hexadecyl chains per molecule. Similarly, dyes **1** and **3** show unmistakable aggregation behavior and colloid formation in highly nonpolar solvents. The nature of the aggregate and spectroscopic properties have not been fully investigated.

*2.3. Electrochemistry of dyes **1–4***

The cyclic voltammetric data was acquired at scan rates from 20 mV s^{-1} to 600 mV s^{-1} of 0.5 mM dyes in dichloromethane (DCM) containing 0.1 M tetrabutylammonium perchlorate (TBAP) as supporting electrolyte. Similar sets of cyclic voltammograms were obtained for all the dyes studied. Data for all the dyes are given in Table 5. The representative voltammograms of dye **4a** are presented in Fig. 7. All three dyes (**3–4b**) show three reduction peaks. These three peaks are equally spaced with the difference of about 230–270 mV in case of dyes **4a** and **4b**, while in case of **3**, the difference is about 530 mV between 1st and 2nd peak and 270 mV between 2nd and 3rd peak.

In some electroactive dendrimers [25–27] containing multiple terpyridyl ruthenium complex and ferrocenyl chromophores only one peak was observed because all units are reduced/oxidized at the same potential. In other words, the potentials are so closely spaced that it was not possible to differentiate them. Since there is only one wave for the reduction process, poor electronic communication

Table 4
Time resolved fluorescence decay of dyes **3**, **4a** and **4b** in organic solvents

Solvents	**3**				**4a**				**4b**			
	τ_1 (ns) (α_1)	τ_2 (ns) (α_2)	τ_{avg} (ns)	χ^2	τ_1 (ns) (α_1)	τ_2 (ns) (α_2)	τ_{avg} (ns)	χ^2	τ_1 (ns) (α_1)	τ_2 (ns) (α_2)	τ_{avg} (ns)	χ^2
MeOH	0.15(0.09)	0.03(0.91)	0.04	1.42	0.34(0.05)	0.1(0.95)	0.11	1.05	0.43(0.21)	0.1(0.79)	0.17	1.26
EtOH	0.18(0.08)	0.05(0.92)	0.06	1.56	0.29(0.26)	0.13(0.74)	0.17	1.07	0.47(0.18)	0.15(0.82)	0.21	0.88
1-Octanol	0.92(0.45)	0.41(0.55)	0.64	1.02	1.38(0.42)	0.38(0.58)	0.8	1.01	1.90(0.41)	0.78(0.59)	1.24	0.89
$CHCl_3$	0.94(0.48)	0.36(0.52)	0.64	1.11	1.46(0.52)	0.33(0.48)	0.92	1.21	1.48(0.42)	0.38(0.58)	0.84	1.22
CH_2Cl_2	0.55(0.31)	0.22(0.69)	0.32	2.13	1.06(0.52)	0.38(0.48)	0.74	1.17	1.01(0.21)	0.38(0.79)	0.52	1.26

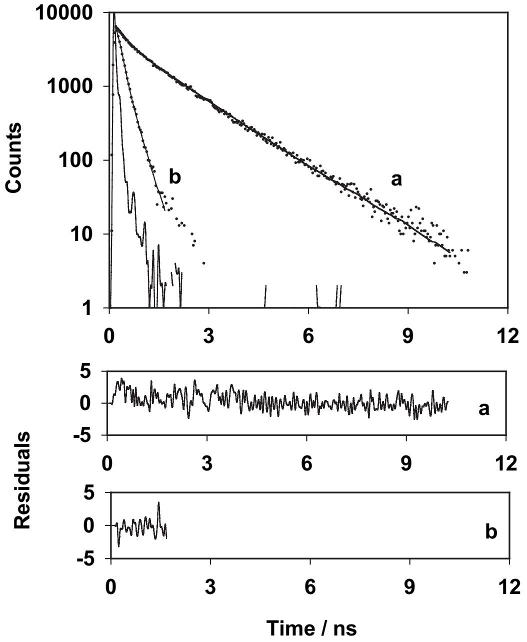

Fig. 5. Time-resolved fluorescence decay of dye **4a** in (a) chloroform and (b) ethanol. The excitation function is also shown. Solid line represents the fitted data. The distribution of weighted residuals is shown in the bottom panels.

among the redox centers is indicated. The tetracationic compounds **1** and **2**, as previously reported [17] (values given in Table 5 for comparison), also show a single broad peak and separation in the peak potentials (34, 20 and 14 mV) was obtained by simulation. Thus, multiple equivalent reduction centers present in these molecules possess weak coupling between the electroactive units. Similarly, it has been seen from the previous study [17] that the monochromophoric dye **M** shows only one sharp formal reduction peak at −1.568 V with respect to Fc^+/Fc due to the monoelectronic reduction of the dye moiety. Therefore, the three reduction peaks in the case of dyes **3** and **4** can be considered as the addition of three successive electrons to the three chromophoric units in the dyes. After addition of one electron to the electroactive unit of **3** or **4**, the second electron addition becomes difficult because of the electronic coupling to the remaining chromophores through the benzene ring. Thus, the peak potential for second electron addition shifts to a higher cathodic value. Similarly, the electronic coupling makes it more difficult to add third electron and the potential shifts further.

In agreement with the earlier reports on some dendritic metal complexes [28,29], it is possible to postulate that the multiple reduction peaks observed for **3–4** is a consequence of intramolecular electronic coupling between the monoreduced chromophore and unreduced chromophore of the dyes. The redox units are separated from one another through an alkyl spacer group in dye **1** and **2** compared to the rigid benzene ring that separates the chromophores in dyes **3** and **4**. This introduces greater conformational rigidity to dyes **3** and **4** as compared to **1** and **2** and permits *greater* electronic communication between the chromophores due to shorter bridging group. This strong electronic communication between the chromophores in **3** and **4** also corroborate with the red shift in absorption spectra vis-à-vis **1** and **2**, respectively.

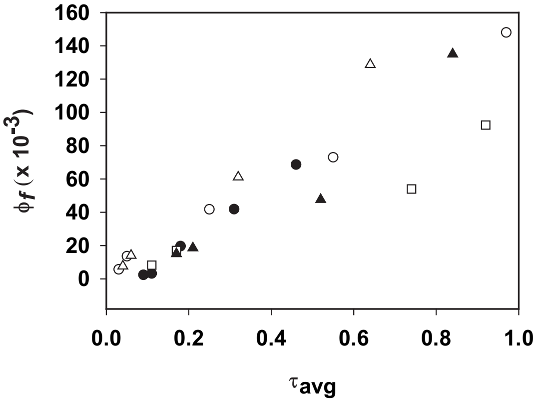

Fig. 6. Plot of fluorescence quantum yield (ϕ_f) vs. average lifetime (τ_{avg}) of dyes **1** (●), **2** (○), **3** (△), **4a** (□) and 4b (▲).

3. Experimental

3.1. General

All solvents (spectroscopic grade) were purchased from E. Merck (India) and used without further purification. All melting points were taken in capillary tubes and are uncorrected. ^1H and ^{13}C NMR spectra were recorded at 500 and 125 MHz, respectively, on a Bruker 500 MHz spectrometer.

Table 5
Cyclic voltammetry data for dyes in DCM at scan rate 0.1 V s^{-1}

Dye	E_{pc1}	E_{pc2}	E_{pc3}	E_{pc4}
	(V) vs. Fc/Fc$^+$			
1[a]	−1.421	−1.455	−1.475	−1.489
2[a]	−1.414	−1.448	−1.468	−1.482
3	−1.356	−1.886	−2.156	–
4a	−1.344	−1.574	−1.844	–
4b	−1.276	−1.55	−1.813	–

[a] Data taken from ref. [17].

J values are given in Hz. Mass spectral data were obtained on a Thermo Finnigan LCQ-Deca series electro spray ion trap mass spectrometer (ESI-MS). Elemental analyses were performed in Theoquest C.E. Instruments EA1112.

The absorption and steady-state fluorescence experiments were recorded using Shimadzu UV2100 and Spex Fluorolog 1681 spectrophotometer, respectively. A concentration of (ca. 1 mM/L) stock solution was prepared separately for each dye by dissolving the required amount of the dye in methanol. The solutions for spectral measurements were prepared by adding the appropriate amount of the dye to maintain its concentration at 10 μM. All measured dye solutions contained 2% MeOH for dyes **1**, **2** and **3** and 2% $CHCl_3$ for **4a** and **4b**, respectively. Aliquots (3 mL) of these solutions were added to quartz cuvettes thermostated at 25 °C. The time-resolved fluorescence measurements were made using a high repetition rate picosecond laser coupled to a time-correlated single photon counting spectrometer described elsewhere, [31] currently using a microchannel plate photomultiplier (Hamamatsu 2809) and a personal computer for data acquisition and analysis. The sample was excited in the blue absorption band of the dye (440 nm) by vertically polarized picosecond laser pulses (frequency doubled Ti-sapphire laser) and the emission was collected (at the peak in 590–625 nm region) through an emission polarizer oriented at the magic angle of 54.7° with respect to the excitation polarization. The FWHM of the instrument response function was approximately 80 ps. Typical photon count rate for fluorescence decay measurements was 4000–5000 s^{-1} (0.1% of the excitation rate) and the typical peak count was 10,000. The fluorescence decays were fitted to biexponential functions by a standard procedure [30].

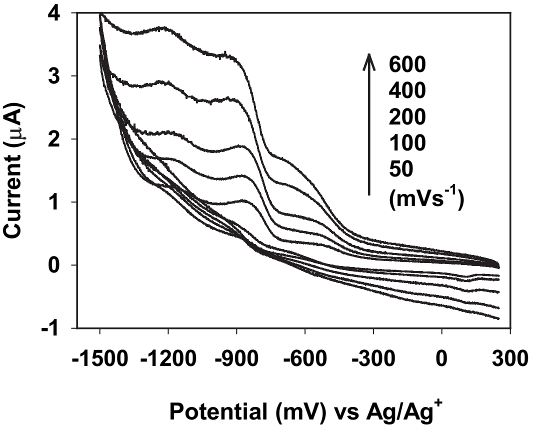

Fig. 7. Overlay of five cyclic voltammograms for 0.5 mM of dye **4a** in DCM, 0.1 M TBAP.

The fluorescence quantum yields (ϕ_f) of the dyes in organic solvents were determined with respect to rhodamine 6G as the standard. The quantum yield of rhodamine 6G in ethanol is 0.95 using excitation wavelength 480 nm [31]. The fluorescence spectrum was corrected for the variation of the quantum efficiency of the photomultiplier (Hamamatsu R928). The quantum yield was calculated using Eq. (1)

$$\phi_{dye} = \phi_{ref}\left(\frac{I_{dye}A_{ref}}{I_{ref}A_{dye}}\right)\left(\frac{\eta_{dye}}{\eta_{ref}}\right)^2 \tag{1}$$

where ϕ_{ref} is the fluorescence quantum yield of rhodamine-6G in ethanol. I_{dye} and I_{ref} are the integrated areas of the corrected fluorescence spectra for the dye and reference, respectively. A_{dye} and A_{ref} are the absorbances of the dye and reference, respectively. η is the refractive index of the solvent [32].

Cyclic voltammetry (CV) experiments were carried out at 25 °C using potentiostat/galvanostat (EG&G PAR, Model 273A), controlled by means of a software loaded into PC. The electrochemical experiments were carried out using a conventional three electrode standard setup 2 cm^3 cell in which a glassy carbon disk electrode (area: 0.06 cm^2), silver wire and Pt gauze were used as the working, quasi-reference and counter electrodes, respectively. The working solution (0.5–1 mM of the electroactive compound + 0.1 M TBAP in dichloromethane) was degassed by bubbling dry argon gas (99.992% purity, iolar grade from BOC India Limited) through it for about 10–15 min prior to each experiment. Before each experiment, the working electrode was carefully polished with 0.05 μ alumina mixed with water. The potential was swept from +0.25 V to −1.5 V and back to +0.25 V with the sweep rate of 100 mV/s to record the current–voltage curve. After each experiment, the glassy carbon electrode was first washed with DCM to dissolve the adsorbed dye on it, then with water and polished as mentioned earlier. Since the silver electrode was used as the pseudo-reference electrode, a second set of voltammograms was obtained after adding a small amount of ferrocene to the solution. The reversible peaks obtained with Fc/Fc$^+$ couple did not interfere with the electrochemistry of the dyes under study and therefore allowed its use as a reference against which, the potentials reported in this work were measured.

3.2. Synthetic procedure

3.2.1. Synthesis of 1,3,5-tris-(hydroxymethyl) benzene (6)

To a stirred solution of 1,3,5-tricarboxybenzene **5** (10 g, 47.6 mmol) in THF (100 mL), under N_2, was added a BH_3·THF solution (1 M; 142.8 mL, 143 mmol) dropwise at 0 °C for 1 h. After the mixture was stirred for 12 h, MeOH (20 mL) was added to quench the reaction, followed by water. The solvents were evaporated in vacuo, aqueous HCl was added, and the mixture was warmed to 60 °C for 1 h to hydrolyze the borate ester formed. The solution was concentrated to dryness and extracted with warm absolute EtOH to give (90%) **6**, as colorless viscous liquid: 7.2 g; ^{1}H (DMSO-d_6) δ 4.49 (6H, s), 5.7 (3H, s), 7.15 (3H, s); ^{13}C (DMSO-d_6) δ 63.47 (CH_2OH), 123.56, 142.45 (C_{Ar}); ESI-MS *m/z* 191.07 $(M+Na)^+$ (calcd. $C_9H_{12}O_3$ 168.07).

3.2.2. Synthesis of 1,3,5-tris-(mesyloxymethyl) benzene (7)

To a stirred solution of triol **6** (5 g, 29.7 mmol) in THF/CH_2Cl_2 (1:1, 50 mL) at 0 °C were added a solution of mesyl chloride (10.5 g, 92.07 mmol) and Et_3N (9.29 g, 92.07 mmol) over 1 h, and then the mixture was maintained at 25 °C for 12 h. The mixture was filtered, giving a filtrate which was evaporated to dryness, and the residue was dissolved in CH_2Cl_2, washed sequentially with water, 10% HCl, $NaHCO_3$, and brine, dried (Na_2SO_4), filtered, and concentrated in vacuo to give a white solid. This crude trimesylate was column chromatographed (SiO_2) eluting with EtOAc/Hex (1:1) to afford (90%) **7**, as white solid: 10.74 g; m.p. 80–83 °C; ^{1}H ($CDCl_3$) δ 2.87 (9H, s), 4.63 (6H, s), 5.74 (3H, s); ^{13}C ($CDCl_3$) δ 36.7 (CH_3), 69.35 (CH_2O), 121.56, 143.23 (C_{Ar}); ESI-MS *m/z* 425.01 $(M+Na)^+$ (calcd. $C_{12}H_{18}O_9S_3$ 402.01).

3.2.3. Synthesis of 1,3,5-tris-(bromomethyl) benzene (8)

To a stirred solution of **7**, (3 g, 7.46 mmol) in DMF (20 mL), excess NaBr (3.81 g, 37 mmol) was added. The mixture was stirred at 60 °C for 4 h. After cooling, the mixture was filtered, evaporated in vacuo to give a solid, which was column chromatographed (SiO_2) eluting with an EtOAc: hexane mixture (1:1) to afford (95%) the desired tetrabromide **8**, as a white solid: 2.52 g; ^{1}H ($CDCl_3$) δ 4.46 (6H, s); 7.37 (3H, s); ^{13}C ($CDCl_3$) δ 32.41 (CH_2Br), 129.75, 139.19 (C_{Ar}); ESI-MS *m/z* 355 $(M+H)^+$ (calcd. $C_9H_9Br_3$ 353.82).

3.2.4. Synthesis of benzene-1,3,5-tris (N,N-dimethylaminostyrylpyridinium bromide) (3)

A mixture of 1,3,5-tris-(bromomethyl)benzene **7**, (500 mg, 1.4 mmol) and γ-picoline (416 mg, 4.5 mmol) in EtOH (10 mL) was refluxed for 8 h. After cooling to 25 °C, the solvent was removed in vacuo giving a residue, which was washed with Et_2O to afford the γ-picolinium salt as white solid. Then *N*,*N*-dimethylaminobenzaldehyde (667 mg, 4.5 mmol) in EtOH (10 mL) and 2–3 drops of piperidine, as catalyst, were added to the salt and then this mixture was refluxed for 5 h. After cooling in an ice bath, the red solid was filtered and then crystallized from MeOH/CH_3CN to afford (60%) the desired dye **3**, as red solid: 860 mg, m.p. 181–183 °C; ^{1}H (CD_3OD) δ 3.38 (18H, s, CH_3), 4.2 (6H, s, CH_2), 5.0–5.4 (br, ArH), 5.6 (3H, d, *J* 16, ethylinic H), 5.9–6.4 (br, ArH), 6.44 (d, *J* 5, ArH), 7.15 (d, *J* 5, ArH); ^{13}C (CD_3OD) δ 39.77 (NCH_3), 59.29 (NCH_2), 112.21, 117.45, 122.72, 122.81, 128.32, 130.51, 142.42, 143.83, 152.15, 153.96 (C_{Ar}); ESI-MS *m/z* (%) 225.4 (100) $[C_{15}H_{17}N_2]^+$, 263.2 (12) $[M - 3Br^-]^{3+}$, 305.4 (26) $[C_{15}H_{16}N_2Br]^+$, 435.2 (40) $[M - 2Br^-]^{2+}$ 748.1 (90) $[M - 305.4 + Na]^+$, 949.9 (14) $[M - Br^-]^+$ (calcd. $C_{54}H_{57}N_6Br_3$; 1029.79). Anal. calcd. for $C_{54}H_{57}N_6Br_3$: C, 62.98; H, 5.58; N, 8.16; found: C, 63.16; H, 5.53; N, 8.32.

3.2.5. *Synthesis of benzene-1,3,5-tris (N,N-dicetylaminostyrylpyridinium bromide) (**4a**)*

Was prepared (70%) by the above procedure by using 1,3,5-tribromomethyl benzene (300 mg, 0.842 mmol), γ-picoline (250 mg, 2.7 mmol) and *N,N*-dihexadecyl aminobenzaldehyde (1.53 g, 4.5 mmol). crystallized from methanol/hexane mixture; 1.35 g, m.p. 247–250 °C; ^1H ($CDCl_3$) δ 0.86 (18H, t, CH_3), 1.26 (aliphatic H, br, s), 1.64 (aliphatic H, m) 3–3.4 (18H, br, m, CH_2), 6.4–6.7 (br, ArH), 6.73 (3H, d, *J* 15, ethylinic H), 6.91, 7.4–7.5 (br, ArH), 7.52 (3H, d, *J* 15, ethylinic H), 7.74 (br, ArH); ^{13}C ($CDCl_3$) δ 14.07 (CH_3), 22.63 (CH_3CH_2), 27.24, 29.33, 29.48, 29.66, 31.88 (CH_2), 51.05 (CH_2NCH_2), 60.1 (br, NCH_2), 111.54, 115.69, 121.47, 122.71, 128.97, 130.90, 142.96, 144.09 150.35, 154.23 (C_{Ar}); ESI-MS *m/z* (%) 646.4 (12) $[C_{45}H_{76}N_2 + H]^+$, 684 (14) $[M - 3Br^-]^{3+}$, 725.9 (100) $[C_{45}H_{76}N_2Br]^+$, 1065.5 (60) $[M - 2Br^-]^{2+}$, 1486.9 (16) $[M - 725.9 - Br^-]^+$, 1566 (12) $[M - 725.9]^+$, 2212.46 (10) $[M - Br^-]^+$ (calcd. $C_{144}H_{237}N_6Br_3$; 2292.22). Anal. calcd. for $C_{144}H_{237}N_6Br_3$: C, 75.45; H, 10.42; N, 3.66; found: C, 75.75; H, 10.36; N, 3.76.

3.2.6. *Synthesis of benzene-1,3,5-tris (N,N-dicetylaminostyrylpyridinium tetraphenylborate) (**4b**)*

To a mixture of **4a** (500 mg, 0.166 mmol) in methanol was added excess of sodium tetraphenylborate (570 mg, 1.66 mmol). The mixture was refluxed for 12 h, after cooling the solvent was evaporated in vacuo and the product was extracted with CH_2Cl_2 to afford **4b** as red solid, crystallized from methanol/hexane mixture, yield quantitative. m.p. 216–219 °C; ^1H ($CDCl_3$) δ 0.88 (18H, t, CH_3), 1.27 (aliphatic H, br, s), 1.63 (aliphatic H, m) 3.1–3.4 (18H, br, m, CH_2), 6.5–7 (br, ArH), 7.1–7.6 (br, ArH); ^{13}C ($CDCl_3$) δ 14.11 (CH_3), 22.69 (CH_3CH_2), 27.14, 29.36, 29.70, 31.93 (CH_2), 51.12 (CH_2NCH_2), 111.75, 115.29, 122.71, 126, 127.15, 128.33, 128.73, 129.64, 130.90, 136.1, 142.14, 154.23 (C_{Ar}); ESI-MS *m/z* (%) 684.2 (6) $[M - 3B(Ph_4)^-]^{3+}$, 726 (100) $[C_{45}H_{76}N_2Ph^- + 2H]^+$, 1185.3 (8) $[M - 2B(Ph_4)^-]^{2+}$, 2691.3 (6) $[M - B(Ph_4)^-]^+$, (calcd. $C_{216}H_{297}N_6B_3$; 3010.23). Anal. calcd for $C_{216}H_{297}N_6B_3$: C, 86.18; H, 9.94; N, 2.79; found: C, 86.36; H, 9.82; N, 3.01.

4. Conclusion

We have synthesised some novel dendritic stilbazolium dyes (a class of hemicyanines) and studied their spectroscopic and electrochemical properties. These dyes show unique solvatochromic behaviour in different solvents. The change in alkyl chain from C1 to C16 shows a red shift in absorption maxima. Systematic variation of fluorescence quantum yield and lifetime in organic solvents were observed. Electrochemical studies have shown three well-separated reduction peaks for dyes **3**, **4a** and **4b** due to a strong electronic coupling between the chromophores, whereas dyes **1** and **2** give only one broad peak. In this study we have shown that, dendritic stilbazolium (hemicyanine) dyes, in which chromophores are electronically communicating, can be constructed with rational design and synthetic approach. This may lead to novel materials with substantial electron mobility and interesting electrical and optical properties for applications in the field of nonlinear optics and optoelectronic devices.

Acknowledgements

AM wishes to express his gratitude to Prof. George R. Newkome, for providing laboratory facilities during his Postdoctoral tenure at Department of Polymer Sciences, University of Akron. We thank Prof. N. Periasamy for his extremely useful and illuminating discussion on time-resolved phenomenon. We thank Ms. M. H. Kombrabail and Dr. A. S. R. Koti for helping in the fluorescence decay measurements of the dyes and Mr. B. T. Kansara for ESI-MS measurements.

References

[1] (a) Mishra A, Behera RK, Behera PK, Mishra BK, Behera GB. Chem Rev 2000;100:1973; (b) Zhu Z. Dyes Pigments 1995;27:77; (c) Rettig W, Majenz W, Lapouyade R, Vogel M. J Photochem Photobiol A 1992;65:95.

[2] (a) Lehn J-M. Supramolecular chemistry. Concepts and perspectives. Weinheim: VCH; 1995; (b) De Silva AP, Gunaratne HQN, Bunnlaugsson T, Huxaley AJM, McCoy CP, Rademacher JT, et al. Chem Rev 1997;97:1515; (c) Gromov SP, Fedorova OA, Ushakov EN, Buevich AV, Baskin II, Pershina YV, et al. J Chem Soc Perkin Trans 1999;2:1323.

[3] (a) Dia ZX, Peng BX. Dyes Pigments 1998;36:169(9); (b) Bach G, Daehne S. Cyanine dyes and related compounds. Rodd's chemistry of carbon compounds. 2nd ed. 2nd Suppl. Amsterdam: Elsevier; 1997. pp. 383–487.

[4] (a) Carpenter MA, Silland CS, Penner TL, Williams DJ, Mukamel SJ. J Phys Chem 1992;96:2810; (b) Clément R, Lacroix P, Evans JSO, O'Hare D. Adv Mater 1994;6:794.

[5] (a) Mishra A, Patel S, Behera RK, Mishra BK, Behera GB. Bull Chem Soc Jpn 1997;70:2913; (b) Mishra A, Behera PK, Behera RK, Mishra BK, Behera GB. J Photochem and Photobiol A 1998;116:79.

[6] (a) Armitage B, O'Brien DF. J Am Chem Soc 1991;113: 9678; (b) Fromherz P, Muller CO. Biochim Biophys Acta 1993;1150:111.

[7] Mishra A, Behera GB, Krishna MMG, Periasamy N. J Luminescence 2001;92:175.

[8] Shibasaki K, Itoh KJ. Raman Spectrosc 1991;22:753.

[9] Cao X, McHale JL. J Chem Phys 1998;109:1901.

[10] Dietz F, Rentsch SK. Chem Phys 1985;96:145.

[11] Ponterini G, Monicchioli F. Chem Phys 1991;151:111.

[12] Mishra A, Behera RK, Fronczek FR, Bidyasagar M, Behera GB. Ind J Chem A 1999;38:982.

[13] Cao X, Tolbert RW, McHale JL, Edwards WD. J Phys Chem A 1998;102:2739.

[14] Huang Y, Cheng T, Li F, Luo C, Huang C-H, Cai Z, et al. J Phys Chem B 2002;106:10031.

[15] Ephardt H, Fromherz P. J Phys Chem 1989;93:7717.

[16] Kim J, Lee M. J Phys Chem A 1999;103:3378.

[17] Mishra A, Newkome GR, Moorefield CN, Godínez LA. Dyes Pigments 2003;58:227.

[18] Lang AD, Huang CH, Gan LB, Zhou DJ. Syn Met 1999;99:97.

[19] (a) Reichardt C, editor. Solvent and solvent effects in organic chemistry. Weinheim: VCH; 1988; (b) Reichardt C. Chem Rev 1994;94:2319.

[20] Fromherz P. J Phys Chem 1995;99:7188.

[21] Gorner H, Gruen H. J Photochem 1985;28:329.

[22] Fromherz P, Heilemann A. J Phys Chem 1992;96:6864.

[23] (a) Yang X, Zaitsev A, Sauerwein B, Murphy S, Schuster GB. J Am Chem Soc 1992;114:793; (b) Murphy S, Schuster GB. J Phys Chem 1995;99:8516.

[24] Song Q, Bohn PW, Blanchard GJ. J Phys Chem B 1997;101:8865.

[25] Goldsmith JI, Takada K, Abruña HD. J Phys Chem B 2002;106:8504.

[26] Takada K, Díaz DJ, Abruña HD, Cuadrado I, Casado C, Alonso B, et al. Am Chem Soc 1997;119:10763.

[27] Nlate S, Ruiz J, Sartor V, Navarro R, Blais J-C, Astruc D. Chem Eur J 2000;6:2544.

[28] Boulas PL, Kaifer MG, Echegoyen L. Angew Chem Int Ed 1998;37:216.

[29] Cuadrado I, Casado CM, Alonso B, Morán M, Losada J, Belsky V. J Am Chem Soc 1997;119:7613.

[30] Periasamy N, Doraiswamy S, Maiya GB, Venkataraman B. J Chem Phys 1988;88:1638.

[31] Kubin RF, Fletcher AN. J Luminescence 1982;27:455.

[32] Su J, Xu T, Chen K, Tian H. Dyes Pigments 2000; 44:87.